

## Thymoquinone Reverses Homocysteine-Induced Endothelial Dysfunction via Inhibition of Endoplasmic Reticulum-Stress Induced Oxidative Stress Pathway (Timoquinon Membalikkan Disfungsi Endotelium Aruhan Homosistein melalui Perencatan Laluan Tekanan Oksidatif Aruhan Retikulum Endoplasma)

SITI SARAH M. SOFIULLAH<sup>1</sup>, DHARMANI DEVI MURUGAN<sup>2</sup>, SUHAILA ABD MUID<sup>3,4</sup>, WU YUAN SENG<sup>5,6</sup>, NOR HISAM ZAMAKSHSHARI<sup>7</sup>, QUAN FU GAN<sup>8</sup>, MELONNEY PATRICK<sup>3,4</sup>, NORASIKIN AB AZIS<sup>9</sup>, SRINIVASA RAO SIRASANAGANDLA<sup>10</sup> & CHOY KER WOON<sup>1,3\*</sup>

<sup>1</sup>Department of Anatomy, Faculty of Medicine, Universiti Teknologi MARA (UiTM), Sungai Buloh Campus, Jalan Hospital, 47000 Sungai Buloh, Petaling Jaya, Selangor, Malaysia

<sup>2</sup>Department of Pharmacology, Faculty of Medicine, Universiti Malaya, 50603 Kuala Lumpur, Malaysia

<sup>3</sup>Institute of Pathology, Laboratory and Forensic Medicine (I-PperForM), Universiti Teknologi MARA (UiTM), Sungai Buloh Campus, Jalan Hospital, 47000 Sungai Buloh, Petaling Jaya, Selangor, Malaysia

<sup>4</sup>Department of Biochemistry and Molecular Medicine, Faculty of Medicine, Universiti Teknologi MARA (UiTM), Sungai Buloh Campus, Jalan Hospital, 47000 Sungai Buloh, Petaling Jaya, Selangor, Malaysia

<sup>5</sup>Sunway Microbiome Centre, School of Medical and Life Sciences, Sunway University, 47500 Subang Jaya, Selangor, Malaysia

<sup>6</sup>Department of Medical Education, School of Medical and Life Sciences, Sunway University, 47500 Subang Jaya, Selangor, Malaysia

<sup>7</sup>Department of Chemistry, Faculty of Resources Science and Technology, University Malaysia Sarawak, Kota Samarahan, 4300, Kuching, Sarawak, Malaysia

<sup>8</sup>Pre-clinical Department, Faculty of Medicine and Health Science, UTAR Sg Long Campus, 43000 Kajang, Selangor, Malaysia

<sup>9</sup>Department of Pharmacology, Faculty of Medicine, Universiti Teknologi MARA (UiTM), Sungai Buloh Campus, Jalan Hospital, 47000 Selangor, Malaysia

<sup>10</sup>Department of Human & Clinical Anatomy, College of Medicine & Health Sciences, Sultan Qaboos University, PO Box 35, PC 123, Al-Khoud, Muscat, Oman

Received: 31 July 2023/Accepted: 9 February 2024

### ABSTRACT

Hyperhomocysteinemia causes endoplasmic reticulum (ER) stress, which elevates reactive oxygen species (ROS) and induces endothelial dysfunction, the hallmark of cardiovascular diseases. *Nigella sativa* seeds contain thymoquinone (TQ), a cardioprotective bioactive component. Nevertheless, research on investigating the effectiveness of TQ in preventing endothelial dysfunction caused by homocysteine (Hcy) is scarce. Therefore, the purpose of this work was to examine the role of TQ in restoring Hcy-induced endothelial dysfunction as well as the mechanisms behind this role. Male Sprague-Dawley (SD) rat aortas were isolated and then co-treated in an organ bath with Hcy and TQ, tauroursodeoxycholic acid (TUDCA), apocynin, or Tempol to examine vascular function. Furthermore, human umbilical vein endothelial cells (HUVECs) were treated with Hcy and TQ, Tempol, apocynin, TUDCA or H<sub>2</sub>O<sub>2</sub> to determine the cell viability via a phase contrast microscope and dye exclusion test. ER stress pathway involvement, ROS and NO bioavailability were investigated using immunoassays and fluorescence staining, respectively. The binding affinity of TQ to GRP78 has been identified using molecular docking. According to our findings, Hcy hindered endothelium-dependent relaxation in an isolated aorta and caused apoptosis in HUVECs. TQ, TUDCA, Tempol, and apocynin were able to counteract these negative effects. In HUVECs, treatment with TQ decreased ROS levels, increased NO bioavailability, and decreased GRP78 and NOX4 protein. According to the molecular docking study outcomes, TQ could attach to GRP78 effectively via a hydrogen bond and a hydrophobic connection to the amino acid at GRP78 ATP binding pocket. Taken together, the findings show that TQ protected endothelial function caused by Hcy via inhibiting ER stress-mediated ROS and eNOS uncoupling.

Keywords: Endoplasmic reticulum stress; endothelial dysfunction; homocysteine; oxidative stress; thymoquinone

## ABSTRAK

Hiperhomosisteinemia meninggikan tekanan retikulum endoplasma (RE) yang boleh meningkatkan spesies oksigen reaktif (SOR), yang membawa kepada disfungsi endotelium sel dan penyakit kardiovaskular. Biji *Nigella sativa* mengandungi timoquinon (TQ), komponen bioaktif berkardio-protektif. Walau bagaimanapun, tiada kajian yang menilai kesan TQ terhadap disfungsi endotelial yang disebabkan oleh homosistein (Hcy). Oleh itu, penyelidikan ini bertujuan untuk mengkaji kesan dan mekanisme TQ dalam menormalkan disfungsi endotelial yang disebabkan oleh Hcy. Aorta diasingkan daripada tikus Sprague-Dawley (SD) jantan yang diinkubasi dengan Hcy dan dirawat bersama dengan atau tanpa TQ, TUDCA, apocynin atau Tempol dalam mandian organ untuk mengkaji fungsi vaskular. Di samping itu, sel endotelial vena umbilik manusia (HUVECs) diinkubasi dengan Hcy dan TQ, Tempol, apocynin, TUDCA atau H<sub>2</sub>O<sub>2</sub> untuk menilai keviabelan sel dengan menggunakan mikroskop kontras fasa dan ujian pengecualian pewarna. Penglibatan laluan tekanan ER, ROS dan NO bioketersediaan diakses masing-masing melalui immunoasai dan pewarnaan pendarfluor. Dok molekul telah dilakukan untuk menilai pertalian mengikat TQ kepada GRP78. Keputusan kami mendedahkan bahawa Hcy merosakkan disfungsi endotelial dalam aorta dan apoptosis dalam HUVECs. Kesan ini telah dinormalkan oleh TQ, TUDCA, Tempol dan apocynin. Rawatan dengan TQ mengurangkan tahap ROS, meningkatkan bioketersediaan NO serta mengurangkan protein GRP78 dan NOX4 dalam HUVECs. Hasil kajian dok molekul menunjukkan bahawa TQ boleh mengikat dengan baik kepada GRP78 melalui ikatan hidrogen dan interaksi hidrofobik dengan asid amino pada poket pengikat ATP GRP78. Kesimpulannya, TQ membaikipulih fungsi endotelial yang dirosakkan oleh Hcy melalui perencatan ROS pengantara tekanan ER dan meningkatkan bioketersediaan NO.

Kata kunci: Disfungsi endotelium; homosistein; tekanan oksidatif; tekanan retikulum endoplasma; timoquinon

## INTRODUCTION

One of the main risk factors for cardiovascular disease is hyperhomocysteinemia (HHcy). Based on data from the World Health Organisation, 17.9 million deaths from cardiovascular disease were reported in 2019. These deaths accounted for 32% of all worldwide fatalities, and 85% of them were due to a heart attack or stroke (Mahadir Naidu et al. 2019). Endothelial dysfunction (ED) is the initial symptom of atherosclerosis and vascular disease. Hcy adversely affects endothelial function, according to various studies (Barroso et al. 2016; Da Silva et al. 2018; Dubey et al. 2022; Kern et al. 2022; Wu et al. 2019; Zhang et al. 2017). Hcy could hinder endothelial-dependent dilatation via oxidative stress, which disrupts nitric oxide (NO) synthase activity uncoupling, endoplasmic reticulum stress (ER stress) and inflammation.

Increased Hcy levels trigger ER stress by interfering with the ER's normal protein folding and processing, which causes a buildup of misfolded proteins via activating the GRP78 protein (Lindholm et al. 2017). Unfolded protein response (UPR) reduces the impact of misfolded proteins by upregulating ER protein folding capacity through enhanced chaperone synthesis and reducing ER protein load through suppression of protein transcription and translation (Amen et al. 2019). This reaction is mediated by three concurrent signal transduction pathways which are inositol requiring enzyme 1 (IRE1), RNA-activated protein kinase-like ER kinase (PERK), and activating transcription factor 6 (ATF6) (Osowski & Urano 2011). Oxidative stress and the ER stress response are subsequently elevated as a result of UPR activation. The role of nicotinamide adenine dinucleotide phosphate

(NADPH) oxidase 4 (NOX4) in the production of reactive oxygen species (ROS) in ER stress-induced disease states has been reported in several investigations (Amanso, Debbas & Laurindo 2011; Loughlin & Artlett 2010; Santos et al. 2009). The availability of nicotinamide adenine dinucleotide phosphate (NADPH), a cofactor for NOX4, regulates NOX4 activity (Vermot et al. 2021). Superoxide radicals (O<sub>2</sub><sup>-</sup>) are created when NADPH binds to NOX4, which causes the enzyme to change in conformation and allows the transfer of electrons from NADPH to molecule oxygen (Sies & Jones 2020). NOX4-mediated ROS production from ER stress can enable the uncoupling of endothelial nitric oxide synthase (eNOS), leading to decreased nitric oxide (NO) formation when O<sub>2</sub><sup>-</sup> interacts rapidly with NO to produce peroxynitrite, another toxic radical, which subsequently results in eNOS to uncouple and discharge additional O<sub>2</sub><sup>-</sup>. Furthermore, ROS can directly deactivate NO via a process called 'oxidation', which reduces NO bioavailability. When NO bioavailability is diminished, the endothelium's ability to initiate and maintain vasodilation is impaired, leading to a reduction in blood flow and an increase in blood pressure. Additionally, decreased NO bioavailability can increase oxidative stress, inflammation, and thrombosis, all of the contributing factors in the development of cardiovascular disease (Medina-Leyte et al. 2021; Panda et al. 2022; Rotariu et al. 2022) These alterations aid in the emergence of endothelial dysfunction, a fundamental component of many cardiovascular illnesses.

There is an unmet need for better clinical outcomes in the treatment of cardiovascular disease. This need can be filled by discovering a novel fundamental mechanism from natural materials that may improve the safety and

effectiveness of treating cardiovascular diseases that are linked to HHcy (Kosmas et al. 2019; Sagud, Tudor & Pivac 2021). The main component of *Nigella sativa* seeds essential oil is (Khader & Eckl 2014) thymoquinone (TQ) or 2-methyl-5-isopropyl-1, 4-benzoquinone (Ahmad et al. 2019; Goyal et al. 2017). Numerous pharmacological actions of TQ, such as its anti-oxidant, anti-microbial, immunomodulatory, anti-inflammatory, anti-histamine, and anti-tumour characteristics, have been examined. (Ammar et al. 2011; Haq et al. 1999; Mansour et al. 2002). The impact and mechanism of TQ on the vascular system, however, are still lacking much research. Consequently, the aim of this study was to identify the vascular effects and cellular mechanisms underpinning the vascular therapeutic role of TQ in Hcy-induced endothelial dysfunction.

## MATERIALS AND METHODS

### ANIMAL PREPARATIONS

The Institutional Animal Care and Use Committee for the Faculty of Medicine at Universiti Malaya gave its permission to all the experimental methods (2018-210807/PHAR/R/DDM (2018/303)). We utilised male Sprague-Dawley (SD) rats that were 8 weeks old and weighed 200-250 g. At the AAALAC-accredited animal experimental unit at the Faculty of Medicine, Universiti Malaya, rats were housed in a room with good ventilation and kept at a constant temperature of 24.1 °C while being given free access to regular rat food and filtered water.

### FUNCTIONAL STUDY

The thoracic aorta was separated from the surrounding connective tissues and fat, cleaned, and cut into rings segments (3-5 mm) before being put in an organ bath with Krebs physiological salt solution after rats were euthanized by CO<sub>2</sub> inhalation (control solution in mM: NaCl 118.93, NaHCO<sub>3</sub> 25.00, MgSO<sub>4</sub> 1.18, KCl 4.69, KH<sub>2</sub>PO 1.03, Glucose 11.10, CaCl<sub>2</sub> 2.38). The solution was kept at 37 °C in an organ bath while being constantly aerated with a gas combination of 95% O<sub>2</sub> and 5% CO<sub>2</sub>. The PowerLab LabChart 6.0 recording device (AD Instruments, NSW, Australia) was used to constantly amplify and record the output from the isometric force-displacement transducers (Grass Instrument Co, Quincy, MA, USA) attached to the rings. Before being stimulated for 15 min with a single high KCl solution (high K<sup>+</sup>, 80 mM) and three times with Krebs solution, the rings were allowed to acclimatise for 45 min under 2.5 g of resting tension. A single exposure to acetylcholine (ACh, 10 μM) was used to induce relaxation after phenylephrine (PE) (1 μM) pre-contraction in order to determine if endothelium was present in the

aortic segments once the tension had stabilised and returned to baseline. The aortic rings were incubated with various concentrations of Hcy (100 μM, 300 μM, 500 μM) for 1 h before producing endothelium-dependent relaxation by cumulative addition of acetylcholine (ACh), which was added from 3 nM to 10 nM. Sodium nitroprusside (SNP), in concentrations ranging from 1 nM to 10 μM, was added to produce the endothelium-independent relaxation. Separate rings were used for each experiment. Another set of experiments was performed in rings incubated with Hcy (500 M) and co-treated with either TQ (Sigma-Aldrich, MO, USA) (0.1 μM, 1 μM, and 10 μM), TUDCA (ER stress inhibitor, 20 μM), apocynin (NOX inhibitor, 10 μM), or Tempol (ROS scavenger, 1 mM) for 1 h in Krebs solution before the generation of endothelial-dependent and -independent relaxation curves (Choy et al. 2017). As a percentage of contraction decrease brought on by PE before administering ACh or SNP separately, concentration-response curves for both endothelium-dependent and -independent relaxation were observed. The maximum effect (R<sub>max</sub>) and the concentration that causes 50% of R<sub>max</sub> were determined using the cumulative concentration-response curves (pEC<sub>50</sub>).

### CELL CULTURE

Human umbilical vein endothelial cells (HUVECs; Lonza, Basel, Switzerland; No. CC-2517) were cultured in endothelial cell medium (ScienCell, USA) with 5% foetal bovine serum (FBS), 1% penicillin, 1% streptomycin, and 1% endothelial cell growth supplement. The cells were grown in a humid environment with 5% CO<sub>2</sub> at a temperature of 37 °C. The cells utilised ranged in passage from 4 to 10. Experiments were conducted when the cells were 90% confluent. For 24 h, the cells were grown in 8 experimental groups (n = 4). The experimental groups are: 1) control 2) Hcy (10 mM) 3) Hcy + thymoquinone (1 μM), 4) Hcy + thymoquinone (10 μM), 5) Hcy + apocynin (NOX inhibitor, 100 μM), 6) Hcy + TUDCA (ER stress inhibitor, 100 μM), 7) Hcy + Tempol (ROS inhibitor, 100 μM), 8) H<sub>2</sub>O<sub>2</sub> (ROS inducer, 200 μM). Based on previously published effective concentration and time values, the concentration (Hcy range from 2 mM to 10 mM, TQ ranged from 1 μM to 40 μM, apocynin 100 μM, TUDCA 100 μM, Tempol 100 μM, H<sub>2</sub>O<sub>2</sub> 200 μM) and time duration (24 h) were selected (Leung et al. 2013; Pai et al. 2021) as well as from our early optimization research.

### CELL VIABILITY

#### *Dye exclusion test*

After being collected with trypsin, the treated HUVECs were centrifuged. 1 mL of media was used to resuspension the cell pellet. After that, 10 μL of the trypan blue/cell

solution was added to a hemacytometer for microscopic observation. Calculations were made for the viable (unstained) and non-viable (stained) cells. The following formula was used to determine the percentage of viable cells:

$$\text{viable cells (\%)} = \frac{\text{total number of viable cells per mL of aliquot} \times \text{dilution factors}}{\text{total number of cells per mL of aliquot}}$$

#### Phase contrast

In 24 well plates, the treated HUVECs were cultivated. After 24 h, phase contrast microscopy was used to analyse the HUVECS' morphological evaluation.

#### DETECTION OF ROS FORMATION IN HUVECS

Dihydroethidium (DHE) dye and confocal microscopy were used to measure the amount of oxidative stress in HUVECs. DHE (5  $\mu\text{M}$ , Invitrogen, Carlsbad, CA, USA) was incubated in a physiological saline solution at room temperature for 15 min with the treated HUVECs, (normal physiological saline solution (NPSS), composition in mM: NaCl 140, KCl 5, CaCl<sub>2</sub> 1, MgCl<sub>2</sub> 1, glucose 10 and HEPES 5) with pH 7.4. Cells were three times washed with NPSS following incubation. Using a 515 nm excitation and a 585 nm long pass filter, the confocal microscope Leica TCS SP5 (Leica Microsystems, Mannheim, Germany) was used to record the intensity of the fluorescence. DHE fluorescence intensity was examined using ImageJ, and the fold change in fluorescence intensity in comparison to the control group was reported.

#### MEASUREMENT OF GRP78 AND NOX4 LEVEL IN HUVECS

##### Protein extraction

HUVECs were extracted for their protein. HUVECs were seeded in 12 well plate and treated with 7 experimental groups (n=4) for 24 h. The cells were washed with PBS three times. The PBS was then replaced with 120  $\mu\text{L}$  radioimmunoprecipitation assay (RIPA) buffer and incubated on ice for 15 min. The cells were spined with a refrigerate centrifuge at 1500 rpm for 30 mins at 4 °C. Supernatant produced were harvested and proceeded with protein determination using enzyme-linked immunosorbent assay (ELISA). The concentration and purity of the total protein were determined based on the ratio of absorbances values obtained at 260 and 280 nm (A260/280) by using a QuickDrop spectrophotometry (Molecular Devices, San Jose, USA). An OD reading range between 0.5 to 0.6 of A260/280 ratio was considered as a pure protein sample for further experiments.

#### Enzyme-linked immunosorbent assay (ELISA): GRP78 and NOX4

ER stress biomarker (GRP78) and ROS biomarker (NOX 4) concentrations were measured using an industry-standard ELISA kit (Elabscience Biotechnology, Wuhan, Hubei, China) in accordance with manufacturer procedure. A microplate reader was used to measure the absorbance at 450 nm (Multiskan FC, ThermoFisher). The expression of GRP78 and NOX4 was represented as fold changes following normalisation to the control, and values are mean  $\pm$  SEM.

#### MEASUREMENT OF NO PRODUCTION IN HUVECS

5  $\mu\text{M}$  of 4-Amino-5-Methylamino-2',7'-Difluorescein (DAF-FM DA; Molecular Probes) was incubated with treated HUVECs for 20 min at 37 °C (Murugan et al. 2020). Next, NPSS was used to rinse the cells, and 5  $\mu\text{M}$  calcium ionophore A23187 was used to activate the cells (SigmaAldrich, St Louis, MO, USA). A microplate reader was used to measure the amount of fluorescence that was excited at 495 nm and emitted at 515 nm. The differences in intracellular NO levels were determined using the relative fluorescence intensity formula (F1/F0), where F0 represents the average fluorescence signals prior to the addition of A23187 and F1 represents the fluorescence signal at certain time intervals after the addition of A23187.

#### MOLECULAR DOCKING STUDY

Using Discovery Studio® 4.0 (Accelrys, San Diego, USA), the 2D structure of thymoquinone was depicted and saved in PDB format. The thymoquinone's shape and energy were then optimised using Avogradr (Hanwell et al. 2012), utilising the steepest descent and conjugated gradient methods, using the MMFF94 force field. GRP78's crystal structure (PDB ID: 5F1X) was downloaded from Protein Data Bank (PDB). Using AutoDockTools, hydrogen atoms were inserted into the structures of both proteins (Morris et al. 2009). AutoDock vina was used for the docking (Eberhardt et al. 2021). The grid box for GRP78 had been established. GRP78 used a grid box that measured 40  $\times$  40  $\times$  40 with 1.0 Å spacing. The iNOS grid box had a 1.0 Å spacing and measured 123.203  $\times$  113.492  $\times$  34.461. To ensure that every residue had an equal opportunity to bind to ligands, the grid box was set to Å 1.0. The binding energies of the docked ligand-binding were ranked. Discovery Studio® 4.0 (Accelrys, San Diego, USA) was used to identify the binding interactions with the greatest binding affinity and to display them. The structure of this ligand was closely examined and evaluated. Redocking of the co-crystallized ligand found in the GRP78



protein structure was carried out to confirm the docking parameters. AutoDock Vina was used for the redocking with the aforementioned parameters.

#### DATA ANALYSIS

Results are shown as the mean  $\pm$  SEM from *n* experiments. Using non-linear regression and the statistical programme GraphPad Prism version 5 (GraphPad Software Inc., San Diego, CA, USA), concentration-response curves were adjusted to a sigmoidal curve. The two-tailed Student's *t*-test was used to compare two groups, and a one-way ANOVA was used, followed by Bonferroni multiple comparison tests, to compare more than two treatments. Statistically significant was defined as  $P < 0.05$ .

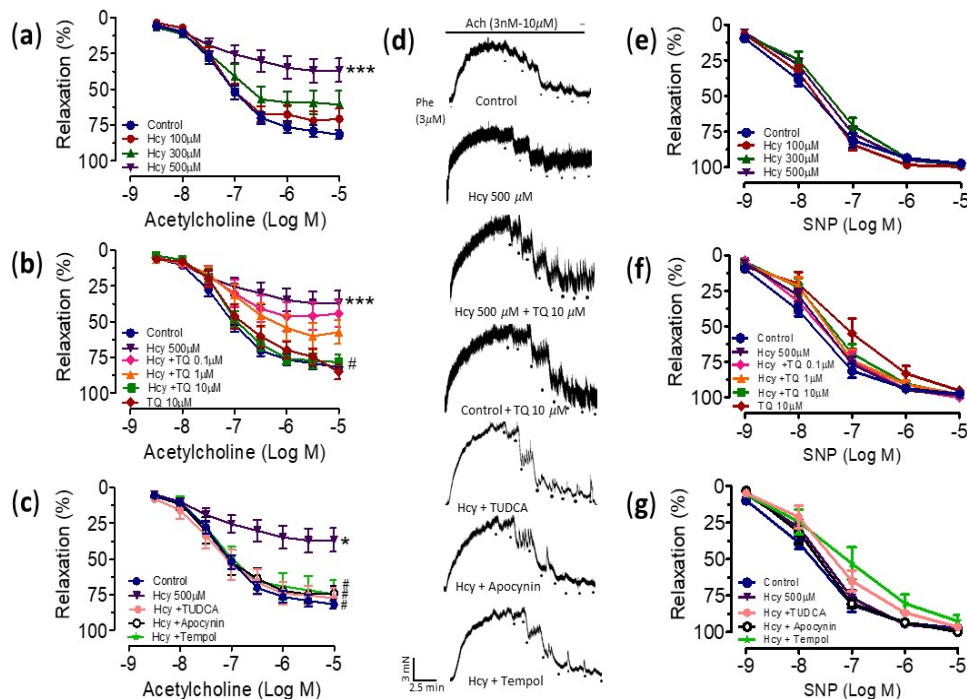
#### RESULTS AND DISCUSSION

##### THYMOQUINONE REVERSES HOMOCYSTEINE-INDUCED ENDOTHELIAL DYSFUNCTION IN ISOLATED RAT AORTA

Rat thoracic aorta rings were incubated in a variety of concentrations of Hcy (100, 300, and 500  $\mu$ M) for 1 hr to

determine the ideal amount of Hcy to inhibit vasorelaxation. In contrast to the control group, 500  $\mu$ M Hcy significantly reduced the ACh-induced vasorelaxation, as seen in Figure 1(a) and 1(b) and Table 1. Endothelial dysfunction in the rat aorta was significantly reversed by co-incubating 500  $\mu$ M Hcy and 10  $\mu$ M TQ for 1 h compared to 500  $\mu$ M Hcy alone (Figure 1(b) and 1(d), Table 1). These findings collectively imply that TQ protected against Hcy-induced endothelial function impairment.

The aortic rings were co-incubated with Hcy (500  $\mu$ M) with 100  $\mu$ M TUDCA (ER stress inhibitor), 100  $\mu$ M Tempol (ROS scavenger), or 100  $\mu$ M apocynin (NOX inhibitor), in order to determine the role of ER stress signalling pathway in the TQ-improved relaxation. The endothelial dysfunction caused by Hcy in the rat aorta was reversed by co-incubating Hcy with TUDCA, apocynin, or Tempol for 1 h, as shown in Figure 1(c) and 1(d) and Table 1. According to these findings, TQ's protective effect against Hcy-induced endothelium dysfunction involves the ER stress pathway. Similar endothelium-independent relaxation elicited by sodium nitroprusside was seen in all treatment groups, indicating that the vascular smooth muscle's sensitivity to NO was unaltered (Figure 1(e)-1(g), Table 1).



Data are presented as means  $\pm$  S.E.M. of (*n*=7) and were analyzed using one-way ANOVA followed by Bonferroni test, non-linear regression and column statistics. \* $p < 0.05$  compared with control, #  $p < 0.05$  compared with Hcy

FIGURE 1. Endothelium-dependent relaxations (a, b & c) induced by acetylcholine, (d) its representative traces and (e, f & g) endothelium-independent relaxations induced by sodium nitroprusside (SNP) of the isolated aorta from SD rats treated with different concentration of Hcy (100  $\mu$ M, 300  $\mu$ M, 500  $\mu$ M), 500  $\mu$ M Hcy co-treated with TQ (0.1  $\mu$ M, 1  $\mu$ M, 10  $\mu$ M), 20  $\mu$ M TUDCA, 100  $\mu$ M apocynin or 1 mM Tempol for 1 h

TABLE 1. Agonist sensitivity (pEC<sub>50</sub>) and percentage of maximum response (R<sub>max</sub>) of endothelium-dependent vasodilator, acetylcholine and endothelium-independent vasodilator sodium nitroprusside (SNP), in isolated aorta from SD rats treated with different concentration of Hcy (100 μM, 300 μM, 500 μM), 500 μM Hcy co-treated with TQ (0.1 μM, 1 μM, and 10 μM), 20 μM TUDCA, 100 μM apocynin or 1 mM Tempol for 1 h

Groups	Acetylcholine		SNP	
	pEC <sub>50</sub> (log M)	Percentage of R <sub>max</sub> (%)	pEC <sub>50</sub> (log M)	Percentage of R <sub>max</sub> (%)
Control	6.190 ± 0.09	81.81 ± 11.18	1.706 ± 0.11	97.55 ± 17.17
Hcy 100 μM	5.105 ± 0.10	72.06 ± 10.35	2.108 ± 0.07	99.72 ± 18.85
Hcy 300 μM	5.456 ± 0.21	60.77 ± 8.03	4.009 ± 0.11	98.56 ± 18.33
Hcy 500 μM	2.753 ± 1.08	37.16 ± 4.39 *	2.758 ± 0.08	98.35 ± 18.59
Hcy 500 μM +TQ 0.1μM	6.017 ± 0.33	46.31 ± 6.02	2.105 ± 0.19	99.96 ± 18.55
Hcy 500 μM + TQ 1μM	1.070 ± 0.26	60.17 ± 7.87	3.660 ± 0.12	97.72 ± 18.60
Hcy 500 μM +TQ 10 μM	7.524 ± 0.09	78.48 ± 11.43 #	3.906 ± 0.12	98.24 ± 18.55
TQ 10 mM	9.411 ± 0.17	85.13 ± 11.05	7.965 ± 0.24	95.11 ± 17.00
Hcy 500 μM + 20 μM TUDCA	4.526 ± 0.25	77.43 ± 9.88 #	4.397 ± 0.16	96.43 ± 18.00
Hcy 500 μM +100 μM apocynin	4.961 ± 0.18	74.90 ± 10.05 #	2.021 ± 0.11	99.80 ± 18.89
Hcy 500 μM + 1 mM Tempol	5.322 ± 0.19	74.66 ± 10.15 #	6.324 ± 0.39	92.52 ± 16.34

Results are mean ± S.E.M. of n=7 experiments, \*p<0.05 compared with control, #p<0.05 compared with Hcy

Based on our findings, TQ has the therapeutic potential to preserve endothelial function by improving endothelium-dependent relaxations, which is comparable to the outcome of incubating TUDCA and apocynin with Hcy. TQ's vasodilatory effects were also shown in different vascular disease models. TQ was found to increase nitrite/nitrate concentrations (NO<sub>x</sub>), increase endothelial nitric oxide synthase (eNOS) activity, and decrease inducible nitric oxide synthase (iNOS) activity in the isolated rabbit aorta, reversing pyrogallol-induced endothelial dysfunction. This finding points to TQ's powerful antioxidant capacity (El-Agamy & Nader 2012).

#### THYMOQUINONE INHIBITS ER STRESS-MEDIATED APOPTOSIS BY HCY IN HUVECS

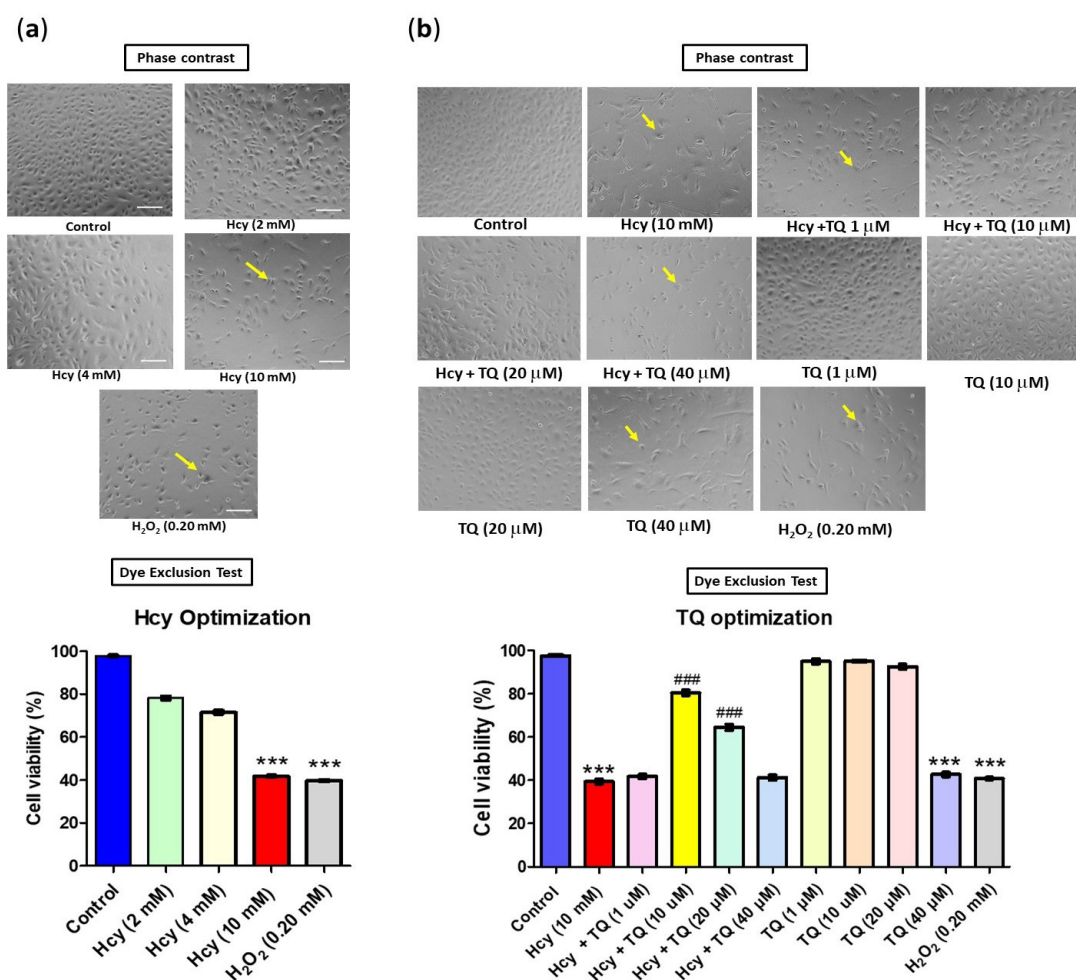
Hcy has been shown to decrease endothelial cell viability when endothelial cells are dysfunctional (Sato et al. 2020; Sipkens et al. 2013; Yuan et al. 2023). Figure 2(a) demonstrates that HUVECS treated with Hcy had reduced cell viability when compared to control in a dose-dependent manner, with 10 mM of Hcy being the most potent concentration that triggered apoptosis when compared to control. Additionally, HUVECS treated with 10 mM of Hcy had altered cell morphology, including cell shrinkage and increased sphericity in comparison to cells in control

groups, which maintained their typical spindle-shaped morphology. The H<sub>2</sub>O<sub>2</sub> treated group, acting as a positive control, differs significantly from the control group as well. Figure 2(b) shows HUVECS co-treated with 10 mM Hcy and TQ of 10 μM and 20 μM has confluent spindle shape/cobblestone morphology, similar in the control group. However, HUVECS co-treated with 10 mM Hcy and 1 μM and 40 μM of TQ showed shrinkage of cells and are more spherical shape indicated by the yellow arrow. Thus, co-treated HUVECS with 10mM Hcy and 10 μM TQ was the most effective concentration that has a significant improvement in the cell viability compared to 10 mM Hcy alone. Figure 2(c) demonstrates that the cell viability of HUVECS co-treated with 10 mM Hcy and 10 μM TQ improved significantly when compared to 10 mM Hcy alone, demonstrating that TQ may restore the cell viability lowered by Hcy. There is no statistically significant difference between treatment with 10 μM TQ alone and control, proving that HUVEC is not harmful at this dose. Additionally, compared to HUVECS co-treated with Hcy and inhibitors (Tempol, TUDCA, and apocynin), co-treatment with Hcy and inhibitors dramatically increased cell viability, which indicates that the normalisation of Hcy-induced apoptosis was accomplished by inhibiting ER stress-mediated ROS. Numerous studies on myocardial, endothelial tissues or cells have found that HHcy causes

an elevation in the production of GRP78 and other proteins involved in mitochondria-ER interaction and apoptosis (Chang et al. 2008; Timkova et al. 2016; Wu et al. 2015). TUDCA, also known as tauroursodeoxycholic acid, is a cytoprotective ER stress inhibitor that has been shown to decrease ER stress as well as the unfolded protein response (UPR) in cells (Reddy et al. 2003). Previous studies demonstrated that TQ functions as an antioxidant, protecting HUVECs from the toxic effects of 2-tert-Butyl-4-hydroquinone (TBHQ) by preventing cell death and lowering apoptosis by reducing DNA and chromatin fragmentation (Karimi et al. 2019).

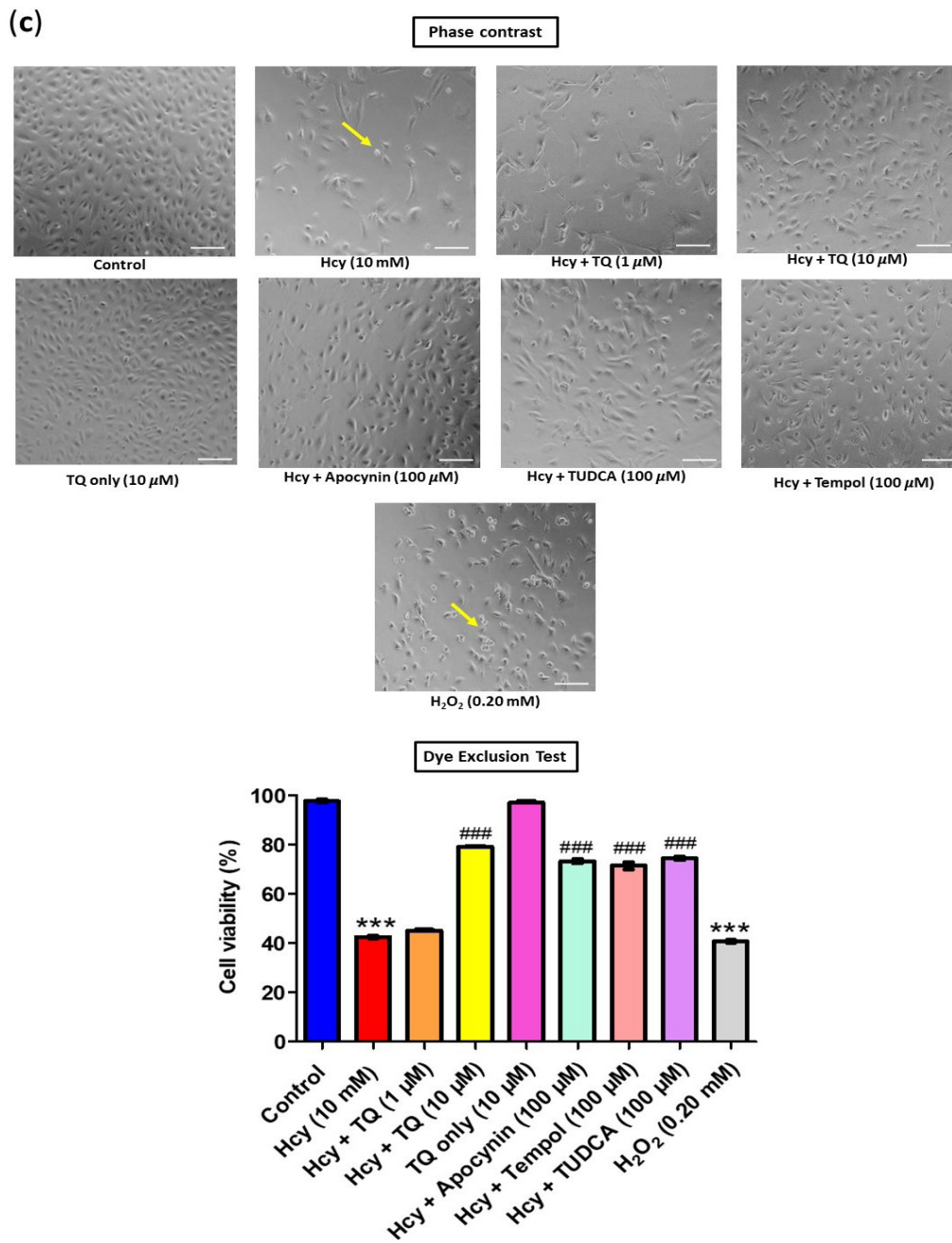
#### THYMOQUINONE REDUCES SUPEROXIDE PRODUCTION INDUCED BY HCY IN HUVECS CELLS

According to several studies, Hcy may enhance ROS production through ER stress by activating the UPR, which raises the expression of NADPH oxidase and ROS-producing enzymes (Kaplan et al. 2020; Ochoa, Wu & Terada 2018; Wu et al. 2019). DHE staining was used to assess intracellular ROS. As shown in Figure 3, our results demonstrate that HUVECS treated for 24 h with Hcy and  $H_2O_2$  had significantly higher DHE fluorescence intensity than the control group. TQ co-treatment decreased the Hcy-stimulated ROS. Our findings further indicate that apocynin and TUDCA reversed the elevated ROS production in HUVECs treated with Hcy. TQ treatment of HUVECs alone did not vary from the control.



Results are mean  $\pm$  S.E.M. of  $n=5$  experiments. \*\*\* $p<0.001$  compared with control ###  $p<0.001$  compared with Hcy. Scale bar represents 100  $\mu$ m. Arrows indicate the cells showing apoptotic cells

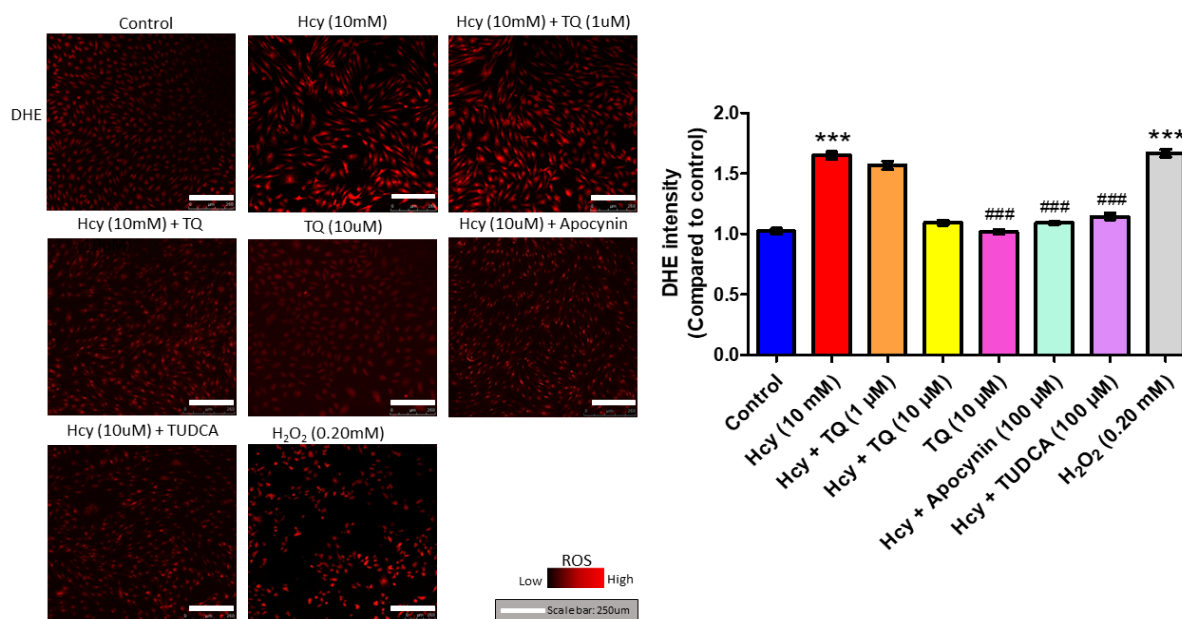
FIGURE 2(a) and 2(b). Phase contrast and dye exclusion test of the effect of HUVECs treated with different concentrations of Hcy (2 mM, 4 mM, and 10 mM) (a), with Hcy (10 mM) and various concentrations of TQ (1, 10, 20 and 40  $\mu$ M) or  $H_2O_2$  (0.20 mM) for 24 h (b)



Results are mean  $\pm$  S.E.M. of  $n=5$  experiments. \*\*\* $p < 0.0015$  compared with control ###  $p < 0.0015$  compared with Hcy. Scale bar represents 100  $\mu\text{m}$ . Arrows indicate the cells showing apoptotic cells

FIGURE 2(c). Phase contrast and dye exclusion test of the effect of HUVECs treated with Hcy (10 mM) and various concentrations of TQ (1  $\mu\text{M}$  and 10  $\mu\text{M}$ ), TQ alone, Tempol (100  $\mu\text{M}$ ), apocynin (100  $\mu\text{M}$ ), TUDCA (100  $\mu\text{M}$ ) or H<sub>2</sub>O<sub>2</sub> (0.20 mM) for 24 h





Results are mean  $\pm$  S.E.M. of n=5 experiments. \*\*\*p<0.001 compared with control ###p<0.001 compared with Hcy. The scale bar represents 250  $\mu$ m

FIGURE 3. Representative images and summarised results of superoxide production measured by DHE fluorescence in HUVECs of all groups

#### THYMOQUINONE NORMALISES GRP78 AND NOX4 PROTEIN EXPRESSION

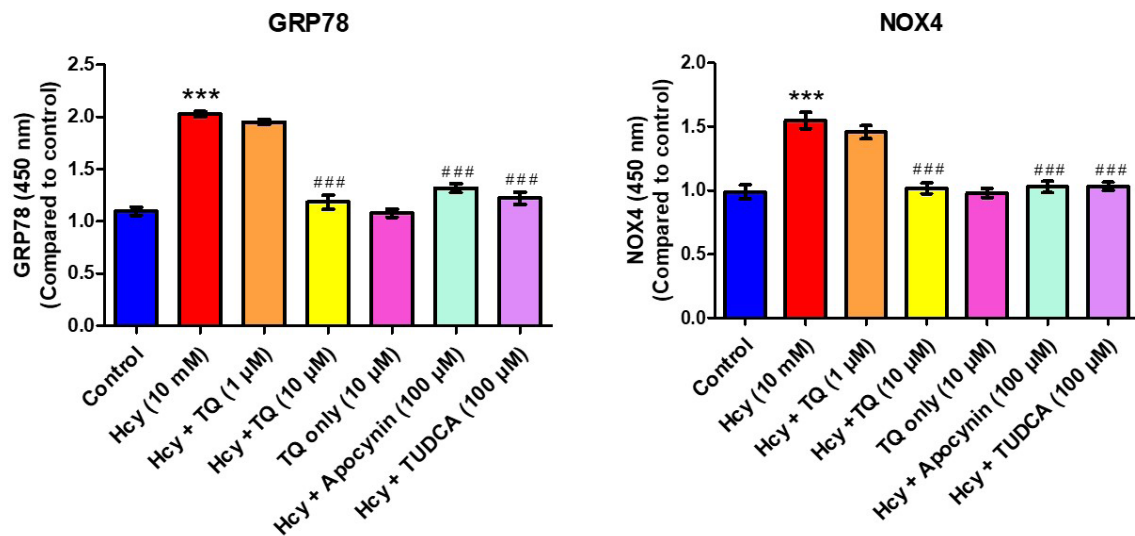
Hcy treatment of HUVECs increased the production of NOX4, which is mostly expressed in mitochondria, activated PERK, increased CHOP, activated NF- $\kappa$ B, and induced apoptosis (Zhang et al. 2017). ELISA was used to assess the level of GRP78 and NOX4 protein expression in HUVECs. HUVECs treated with Hcy elevated GRP78 and NOX4 levels, which were reduced by co-incubating with 10  $\mu$ M of TQ, comparable to the positive control group of TUDCA and apocynin (Figure 4). HUVECS was not affected differently from the control when treated with 10  $\mu$ M of TQ alone. An earlier study showed that TQ changed GRP78 signalling to suppress the pro-apoptotic effects of cisplatin. In ailing liver tissues, TQ increased CHOP-mediated apoptosis while lowering GRP78 levels. HUVECS was not affected differently from the control when treated with 10  $\mu$ M of TQ alone. Previous research showed TQ altered GRP78 signalling to reduce the pro-apoptotic effects of cisplatin. TQ increased CHOP-mediated apoptosis and lowered GRP78 levels in damaged liver tissues (Farghaly et al. 2022). TQ has also been shown to be a potential drug for the treatment of ventricular hypertrophy since it prevents the condition by reducing NOX4 in an AMPK-dependent way (Chen et al. 2022).

#### THYMOQUINONE IMPROVES THE BIOAVAILABILITY OF NO IN HUVECS

Hcy increased superoxide, which decreased the amount of NO available in the coronary artery endothelium of rats, impairing flow-induced coronary artery dilations (Ungvari et al. 2002). TQ is helpful in treating pyrogallol-induced endothelial dysfunction in isolated rabbit aorta because it increases nitrate concentrations while decreasing iNOS activity (El-Agamy & Nader 2012). DAF-FM DA staining was used to assess NO bioavailability in HUVECs. Our most recent data supports these results; HUVECS treated with 10 mM of Hcy and H<sub>2</sub>O<sub>2</sub> reduced NO generation, which was normalised by co-incubation with 10  $\mu$ M of TQ, similarly to the positive control group of apocynin and TUDCA (Figure 5). HUVECS was not significantly different from the control when treated with 10  $\mu$ M of TQ on its own.

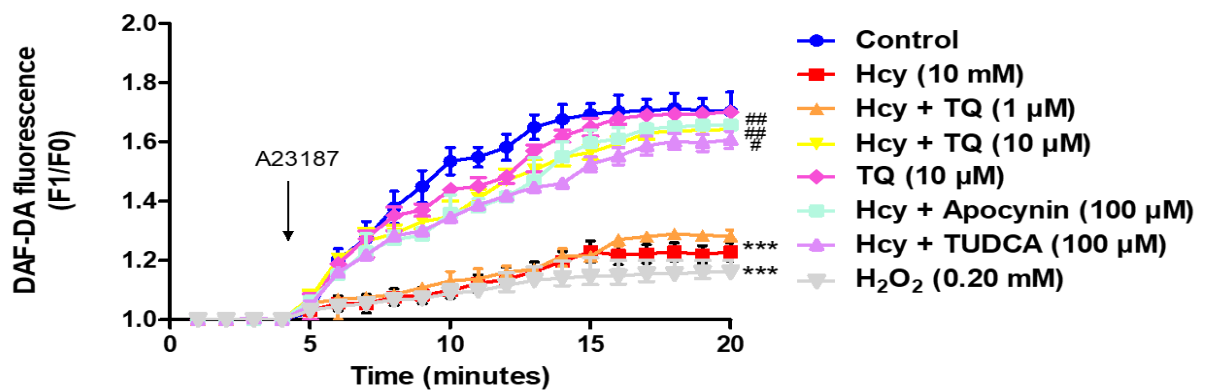
#### MODELLING OF THYMOQUINONE INTO THE ATP-BINDING POCKET OF GRP78

The root means square derivative (RMSD) value between the co-crystallized ligand crystal pose and the top-ranked docked ligand conformation of co-crystallized ligand was determined to be 0.2335 Å (Figure 6(a) and 6(b)). It was



Results are mean  $\pm$  S.E.M. of n=5 experiments. \*\*\*p<0.001 compared with control ###p<0.001 compared with Hcy

FIGURE 4. Measurement of GRP78 (ER stress marker) and NOX 4 (NOX marker) in HUVECs by ELISA



Results are mean  $\pm$  S.E.M. of n=5 experiments. \*p<0.05 compared with control #p<0.05 compared with Hcy, \*\*p<0.01 compared with control, ##p<0.01 compared with Hcy, \*\*\*p<0.001 compared with control, ###p<0.001 compared with Hcy

FIGURE 5. NO bioavailability is increased in HUVEC by thymoquinone. Result of 4-amino-5-methylamino-2', 7'-dichlorofluorescein (DAF-FM) which measures NO production before and after addition of calcium ionophore A23187 (1 μM) for 20 min in HUVEC incubated with Hcy (10 mM) and various concentrations of TQ (1 μM and 10 μM) or H<sub>2</sub>O<sub>2</sub> (0.20 mM), and different inhibitors of apocynin (100 μM) or TUDCA (100 μM) for 24 h

found that the docked inhibitor conformation from the redocking investigation had a comparable orientation to the crystallised inhibitor in the crystal structure, indicating that AutoDock Vina has good accuracy in predicting the binding interactions of the target ligand with crystal structure (Al-Madhagi et al. 2019). The goal of the molecular docking was to determine how thymoquinone physically inhibits GRP78. Thymoquinone was discovered to have a strong affinity for GRP78, with a binding energy of -6.5 kcal/mol. In order to compare how thymoquinone and GRP78 bind to each other, critical residues in the ATP-binding site were identified and utilised as a guide. The residues are ASP34, GLY36, THR37, THR38, TYR39,

ILE61, LYS96, ASP224, GLY226, GLY22, GLY228, THR229, ASP231, GLY 255, GLU256, GLU293, LYS296, ARG297, SER300, GLY363, GLY364, SER365, ARG367, ILE368 and ASP391 which agreed with Allam et al. (2020). Thirteen residues were engaged in the binding interaction between thymoquinone. In the ATP-binding site, every residue is comparable to a critical residue. The main factor contributing to the inhibitory action was intended to be the hydrogen bond between thymoquinone and the THR37, THR38, and TYR39 binding pockets (Figure 6(c) and 6(d)). The results of the *in silico* investigation support the *in vitro* results that revealed TQ decreased GRP78 level.

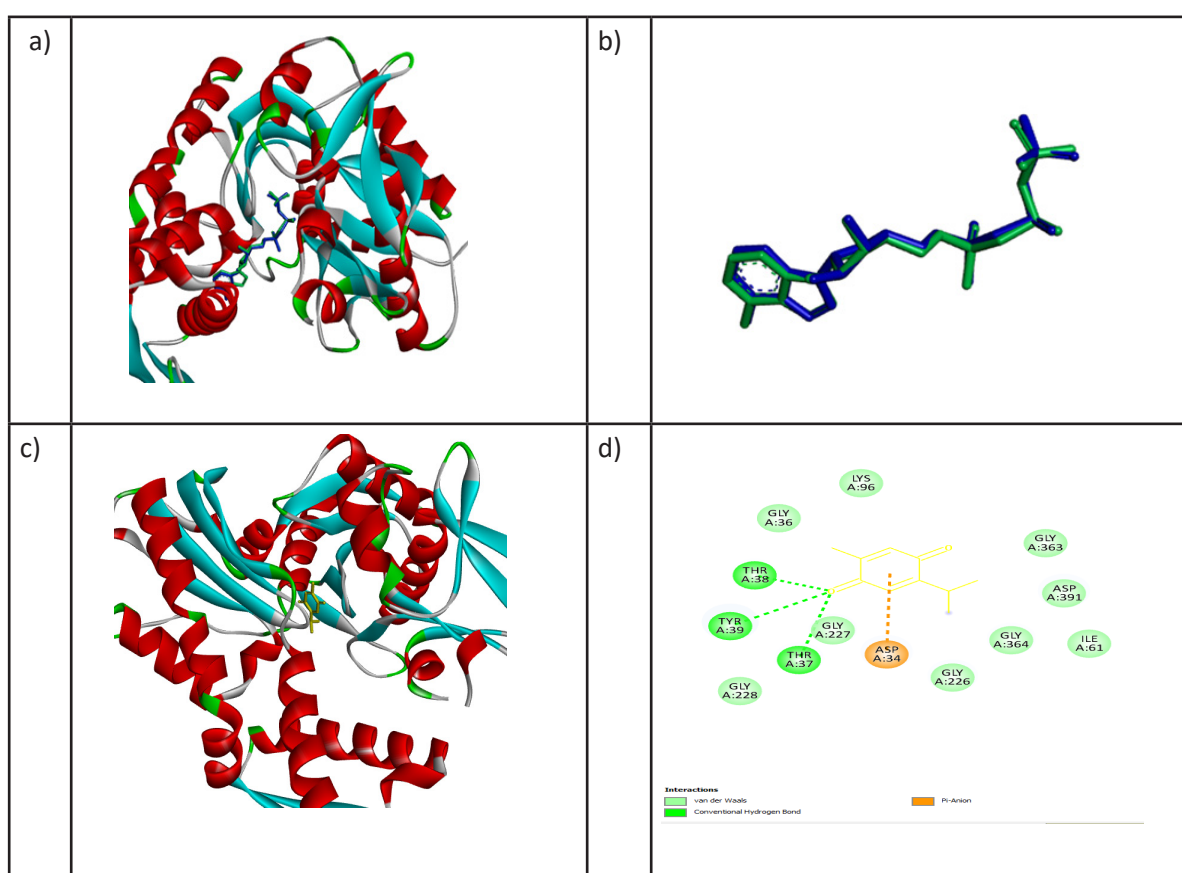


FIGURE 6. Diagrams showing (a) the alignment of the redocked co-crystallised structure, (green stick model) and co-crystallised (Blue stick model) within the binding site of GRP78; (b) superimposition of redocking co-crystalise structure (green stick model) and co-crystallised structure (yellow stick model); (c) thymoquinone (yellow stick model) within the ATP binding pocket of GRP78; d) The 2D schematic diagram of residues in the binding site of GRP78 exhibiting hydrogen bond and hydrophobic interaction with co-crystallised ligand visualised and analysed by using Discovery studio 4.0

## CONCLUSIONS

In conclusion, the present results indicated that TQ reduced Hcy-induced endothelial dysfunction, most likely by lowering the expression of GRP78 and NOX4, which in turn reduces ER stress and, as a result, lowers ROS overproduction and restores NO bioavailability. Thus, the significance of our study is it can be the platform for future *in-vivo* studies and human trials to address the vascular protective and mechanisms of TQ. The current findings provide additional evidence for using TQ as a natural and potent antioxidant drug that may prevent endothelial dysfunction caused by ER stress cardiovascular diseases in the future. Moreover, this study helps to reduce economic burden by providing a more cost-effective adjunct therapy with the aim to prevent CVD and provide pilot reference for future large-scale work to be formulated and marketed as an alternative treatment for HHcy-induced ED in CVD.

## LIMITATIONS

The results of the current study support the use of TQ in the prevention of Hcy-induced endothelial dysfunction. However, we humbly admit that there are some limitations of the study. Our study focused on endothelial-dependent relaxation effects. To further understand the role of TQ in enhancing endothelial function, future research involving endothelium-dependent contractions should be included.

Other variables that limited the scope of this investigation included time and financial restrictions. These restrictions made it challenging for our research team to proceed with an *in-vivo* study before a human trial to support the vascular protection properties of TQ. Future research should thus focus on designing *in-vivo* and clinical investigations as well as effectiveness and safety trials to verify our early findings and identify the ideal dose that provides vascular protection effects while assuring safety from any side effects.

## ACKNOWLEDGEMENTS

This research was funded by Geran Penyelidikan Khas (GPK) Universiti Teknologi MARA: 600-RMC/GPK 5/3 (269/2020) and Geran Insentif Penyelidikan (GIP) Fasa 3/2021, Universiti Teknologi MARA: 600-RMC/GIP 5/3 (079/2021).

## REFERENCES

Ahmad, A., Mishra, R.K., Vyawahare, A., Kumar, A., Rehman, M.U., Qamar, W., Khan, A.Q. & Khan, R. 2019. Thymoquinone (2-Isoprpyl-5-methyl-1, 4-benzoquinone) as a chemopreventive/anticancer agent: Chemistry and biological effects. *Saudi Pharm. J.* 27(8): 1113-1126. doi:10.1016/j.jsps.2019.09.008

- Al-Madhagi, W.M., Hashim, N.M., Awadh Ali, N.A., Taha, H., Alhadi, A.A., Abdullah, A.A., Sharhan, O. & Othman, R. 2019. Bioassay-guided isolation and *in silico* study of antibacterial compounds from petroleum ether extract of *Peperomia blanda* (Jacq.) Kunth. *J. Chem. Inf. Model* 59(5): 1858-1872. doi:10.1021/acs.jcim.8b00969
- Allam, L., Ghrifi, F., Mohammed, H., El Hafidi, N., El Jaoudi, R., El Harti, J., Lmimouni, B., Belyamani, L. & Ibrahimi, A. 2020. Targeting the GRP78-dependant SARS-CoV-2 cell entry by peptides and small molecules. *Bioinform. Biol. Insights* 14: 1177932220965505. doi:10.1177/1177932220965505
- Amanso, A.M., Debbas, V. & Laurindo, F.R. 2011. Proteasome inhibition represses unfolded protein response and Nox4, sensitizing vascular cells to endoplasmic reticulum stress-induced death. *PLoS ONE* 6(1): e14591.
- Amen, O.M., Sarker, S.D., Ghildyal, R. & Arya, A. 2019. Endoplasmic reticulum stress activates unfolded protein response signaling and mediates inflammation, obesity, and cardiac dysfunction: Therapeutic and molecular approach. *Frontiers in Pharmacology* 10. doi:10.3389/fphar.2019.00977
- Ammar, E-S.M., Gameil, N.M., Shawky, N.M. & Nader, M.A. 2011. Comparative evaluation of anti-inflammatory properties of thymoquinone and curcumin using an asthmatic murine model. *International Immunopharmacology* 11(12): 2232-2236.
- Barroso, M., Kao, D., Blom, H.J., de Almeida, I.T., Castro, R., Loscalzo, J. & Handy, D.E. 2016. S-adenosylhomocysteine induces inflammation through NFkB: A possible role for EZH2 in endothelial cell activation. *Biochimica et Biophysica Acta (BBA)-Molecular Basis of Disease* 1862(1): 82-92.
- Chang, L., Geng, B., Yu, F., Zhao, J., Jiang, H., Du, J. & Tang, C. 2008. Hydrogen sulfide inhibits myocardial injury induced by homocysteine in rats. *Amino Acids* 34: 573-585.
- Chen, H., Zhuo, C., Zu, A., Yuan, S., Zhang, H., Zhao, J. & Zheng, L. 2022. Thymoquinone ameliorates pressure overload-induced cardiac hypertrophy by activating the AMPK signalling pathway. *Journal of Cellular and Molecular Medicine* 26(3): 855-867.
- Choy, K.W., Lau, Y.S., Murugan, D. & Mustafa, M.R. 2017. Chronic treatment with paeonol improves endothelial function in mice through inhibition of endoplasmic reticulum stress-mediated oxidative stress. *PLoS ONE* 12(5): e0178365. doi:10.1371/journal.pone.0178365
- Da Silva, I.V., Barroso, M., Moura, T., Castro, R. & Soveral, G. 2018. Endothelial aquaporins and hypomethylation: Potential implications for atherosclerosis and cardiovascular disease. *International Journal of Molecular Sciences* 19(1): 130.



- Dubey, G.P., Jain, D., Mishra, V.N., Dubey, S., Ojha, A. & Kesharwani, R.K. 2022. Homocysteine-mediated endothelial dysfunction in metabolic syndrome. In *Homocysteine Metabolism in Health and Disease*, edited by Dubey, G.P., Misra, K., Kesharwani, R.K. & Ojha, R.P. Springer. pp. 51-70.
- Eberhardt, J., Santos-Martins, D., Tillack, A.F. & Forli, S. 2021. AutoDock Vina 1.2.0: New docking methods, expanded force field, and python bindings. *J. Chem. Inf. Model* 61(8): 3891-3898. doi:10.1021/acs.jcim.1c00203
- El-Agamy, D.S. & Nader, M.A. 2012. Attenuation of oxidative stress-induced vascular endothelial dysfunction by thymoquinone. *Experimental Biology and Medicine* 237(9): 1032-1038.
- Farghaly, M.E., Khowailed, A.A., Aboulhoda, B.E., Rashed, L.A., Gaber, S.S. & Ashour, H. 2022. Thymoquinone potentiated the anticancer effect of cisplatin on hepatic tumorigenesis by modulating tissue oxidative stress and endoplasmic GRP78/CHOP signaling. *Nutr. Cancer* 74(1): 278-287. doi:10.1080/01635581.2021.1879880
- Goyal, S.N., Prajapati, C.P., Gore, P.R., Patil, C.R., Mahajan, U.B., Sharma, C., Talla, S.P. & Ojha, S.K. 2017. Therapeutic potential and pharmaceutical development of thymoquinone: A multitargeted molecule of natural origin. *Frontiers in Pharmacology* 8: 656. doi:10.3389/fphar.2017.00656
- Hanwell, M.D., Curtis, D.E., Loni, D.C., Vandermeersch, T., Zurek, E. & Hutchison, G.R. 2012. Avogadro: An advanced semantic chemical editor, visualization, and analysis platform. *Journal of Cheminformatics* 4(1): 17. doi:10.1186/1758-2946-4-17
- Haq, A., Lobo, P.I., Al-Tufail, M., Rama, N.R. & Al-Sedairy, S.T. 1999. Immunomodulatory effect of *Nigella sativa* proteins fractionated by ion exchange chromatography. *International Journal of Immunopharmacology* 21(4): 283-295.
- Kaplan, P., Tatarkova, Z., Sivonova, M.K., Racay, P. & Lehotsky, J. 2020. Homocysteine and mitochondria in cardiovascular and cerebrovascular systems. *Int. J. Mol. Sci.* 21(20): 7698. doi:10.3390/ijms21207698
- Karimi, Z., Ghaffari, M., Ezzati Nazhad Dolatabadi, J. & Dehghan, P. 2019. The protective effect of thymoquinone on tert-butylhydroquinone induced cytotoxicity in human umbilical vein endothelial cells. *Toxicol. Res. (Camb)* 8(6): 1050-1056. doi:10.1039/c9tx00235a
- Kern, K., Sinnigen, K., Engemann, L., Maiß, C., Hanusch, B., Mügge, A., Lücke, T. & Brüne, M. 2022. Homocysteine as a potential indicator of endothelial dysfunction and cardiovascular risk in female patients with borderline personality disorder. *Borderline Personality Disorder and Emotion Dysregulation* 9(1): 1-9.
- Khader, M. & Eckl, P.M. 2014. Thymoquinone: An emerging natural drug with a wide range of medical applications. *Iran J. Basic Med. Sci.* 17(12): 950-957.
- Kosmas, C.E., Sourlas, A., Silverio, D., Montan, P.D. & Guzman, E. 2019. Novel lipid-modifying therapies addressing unmet needs in cardiovascular disease. *World J. Cardiol.* 11(11): 256-265. doi:10.4330/wjc.v11.i11.256
- Leung, S.B., Zhang, H., Lau, C.W., Huang, Y. & Lin, Z. 2013. Salidroside improves homocysteine-induced endothelial dysfunction by reducing oxidative stress. *Evid. Based Complement Alternat. Med.* 2013: 679635. doi:10.1155/2013/679635
- Lindholm, D., Korhonen, L., Eriksson, O. & Kōks, S. 2017. Recent insights into the role of unfolded protein response in ER stress in health and disease. *Frontiers in Cell and Developmental Biology* 5: 48. doi:10.3389/fcell.2017.00048
- Loughlin, D.T. & Artlett, C.M. 2010. Precursor of advanced glycation end products mediates ER-stress-induced caspase-3 activation of human dermal fibroblasts through NAD(P)H oxidase 4. *PLoS ONE* 5(6): e11093.
- Mahadir Naidu, B., Mohd Yusoff, M.F., Abdullah, S., Musa, K.I., Yaacob, N.M., Mohamad, M.S., Sahril, N. & Aris, T. 2019. Factors associated with the severity of hypertension among Malaysian adults. *PLoS ONE* 14(1): e0207472. doi:10.1371/journal.pone.0207472
- Mansour, M.A., Nagi, M.N., El-Khatib, A.S. & Al-Bekairi, A.M. 2002. Effects of thymoquinone on antioxidant enzyme activities, lipid peroxidation and DT-diaphorase in different tissues of mice: A possible mechanism of action. *Cell Biochemistry and Function* 20(2): 143-151.
- Medina-Leyte, D.J., Zepeda-García, O., Domínguez-Pérez, M., González-Garrido, A., Villarreal-Molina, T. & Jacobo-Albavera, L. 2021. Endothelial dysfunction, inflammation and coronary artery disease: Potential biomarkers and promising therapeutic approaches. *Int. J. Mol. Sci.* 22(8): 3850. doi:10.3390/ijms22083850
- Morris, G.M., Huey, R., Lindstrom, W., Sanner, M.F., Belew, R.K., Goodsell, D.S. & Olson, A.J. 2009. AutoDock4 and AutoDockTools4: Automated docking with selective receptor flexibility. *J. Comput. Chem.* 30(16): 2785-2791. doi:10.1002/jcc.21256
- Murugan, D.D., Md Zain, Z., Choy, K.W., Zamakshshari, N.H., Choong, M.J., Lim, Y.M. & Mustafa, M.R. 2020. Edible bird's nest protects against hyperglycemia-induced oxidative stress and endothelial dysfunction. *Frontiers in Pharmacology* 10: 1624. doi:10.3389/fphar.2019.01624
- Ochoa, C.D., Wu, R.F. & Terada, L.S. 2018. ROS signaling and ER stress in cardiovascular disease. *Molecular Aspects of Medicine* 63: 18-29. doi:https://doi.org/10.1016/j.mam.2018.03.002

- Osowski, C.M. & Urano, F. 2011. Measuring ER stress and the unfolded protein response using mammalian tissue culture system. *Methods Enzymol.* 490: 71-92. doi:10.1016/b978-0-12-385114-7.00004-0
- Pai, P.-Y., Chou, W.-C., Chan, S.-H., Wu, S.-Y., Chen, H.-I., Li, C.-W., Hsieh, P.-L., Chu, P.-M., Chen, Y.-A., Ou, H.-C. & Tsai, K.-L. 2021. Epigallocatechin gallate reduces homocysteine-caused oxidative damages through modulation SIRT1/AMPK pathway in endothelial cells. *The American Journal of Chinese Medicine* 49(01): 113-129.
- Panda, P., Verma, H.K., Lakkakula, S., Merchant, N., Kadir, F., Rahman, S., Jeffree, M.S., Lakkakula Bhaskar, V.K.S. & Rao, P.V. 2022. Biomarkers of oxidative stress tethered to cardiovascular diseases. *Oxidative Medicine and Cellular Longevity* 2022: 9154295. doi:10.1155/2022/9154295
- Reddy, R.K., Mao, C., Baumeister, P., Austin, R.C., Kaufman, R.J. & Lee, A.S. 2003. Endoplasmic reticulum chaperone protein GRP78 protects cells from apoptosis induced by topoisomerase inhibitors: Role of ATP binding site in suppression of caspase-7 activation. *J. Biol. Chem.* 278(23): 20915-20924. doi:10.1074/jbc.M212328200
- Rotariu, D., Babes, E.E., Tit, D.M., Moisi, M., Bustea, C., Stoicescu, M., Radu, A.-F., Vesa, C.M., Behl, T., Bungau, A.F. & Bungau, S.G. 2022. Oxidative stress – Complex pathological issues concerning the hallmark of cardiovascular and metabolic disorders. *Biomedicine & Pharmacotherapy* 152: 113238. doi:https://doi.org/10.1016/j.biopha.2022.113238
- Sagud, M., Tudor, L. & Pivac, N. 2021. Personalized treatment interventions: nonpharmacological and natural treatment strategies in Alzheimer's disease. *Expert Review of Neurotherapeutics* 21(5): 571-589. doi:10.1080/14737175.2021.1906223
- Santos, C.X., Tanaka, L.Y., Wosniak Jr., J. & Laurindo, F.R. 2009. Mechanisms and implications of reactive oxygen species generation during the unfolded protein response: Roles of endoplasmic reticulum oxidoreductases, mitochondrial electron transport, and NADPH oxidase. *Antioxidants & Redox Signaling* 11(10): 2409-2427.
- Sato, K., Nishii, T., Sato, A. & Tatsunami, R. 2020. Autophagy activation is required for homocysteine-induced apoptosis in bovine aorta endothelial cells. *Heliyon* 6(1): e03315. doi:https://doi.org/10.1016/j.heliyon.2020.e03315
- Sies, H. & Jones, D.P. 2020. Reactive oxygen species (ROS) as pleiotropic physiological signalling agents. *Nature Reviews Molecular Cell Biology* 21(7): 363-383. doi:10.1038/s41580-020-0230-3
- Sipkens, J.A., Hahn, N., van den Brand, C.S., Meischl, C., Cillessen, S.A., Smith, D.E.C., Juffermans, L.J.M., Musters, R.J.P., Roos, D., Jakobs, C., Blom, H.J., Smulders, Y.M., Krijnen, P.A.J., Stehouwer, C.D.A., Rauwerda, J.A., van Hinsbergh, V.W.M. & Niessen, H.W.M. 2013. Homocysteine-induced apoptosis in endothelial cells coincides with nuclear NOX2 and peri-nuclear NOX4 activity. *Cell Biochem. Biophys.* 67(2): 341-352. doi:10.1007/s12013-011-9297-y
- Timkova, V., Tatarkova, Z., Lehotsky, J., Racay, P., Dobrota, D. & Kaplan, P. 2016. Effects of mild hyperhomocysteinemia on electron transport chain complexes, oxidative stress, and protein expression in rat cardiac mitochondria. *Molecular and Cellular Biochemistry* 411: 261-270.
- Ungvari, Z., Csiszar, A., Bagi, Z. & Koller, A. 2002. Impaired nitric oxide-mediated flow-induced coronary dilation in hyperhomocysteinemia: Morphological and functional evidence for increased peroxynitrite formation. *Am. J. Pathol.* 161(1): 145-153. doi:10.1016/s0002-9440(10)64166-1
- Vermot, A., Petit-Härtlein, I., Smith, S.M.E. & Fieschi, F. 2021. NADPH oxidases (NOX): An overview from discovery, molecular mechanisms to physiology and pathology. *Antioxidants (Basel)* 10(6): 890. doi:10.3390/antiox10060890
- Wu, S., Gao, X., Yang, S., Meng, M., Yang, X. & Ge, B. 2015. The role of endoplasmic reticulum stress in endothelial dysfunction induced by homocysteine thiolactone. *Fundamental & Clinical Pharmacology* 29(3): 252-259.
- Wu, X., Zhang, L., Miao, Y., Yang, J., Wang, X., Wang, C.-C., Feng, J. & Wang, L. 2019. Homocysteine causes vascular endothelial dysfunction by disrupting endoplasmic reticulum redox homeostasis. *Redox Biology* 20: 46-59.
- Yuan, D., Chu, J., Lin, H., Zhu, G., Qian, J., Yu, Y., Yao, T., Ping, F., Chen, F. & Liu, X. 2023. Mechanism of homocysteine-mediated endothelial injury and its consequences for atherosclerosis. *Frontiers in Cardiovascular Medicine* 9: 1109445. doi:10.3389/fcvm.2022.1109445
- Zhang, Z., Wei, C., Zhou, Y., Yan, T., Wang, Z., Li, W. & Zhao, L. 2017. Homocysteine induces apoptosis of human umbilical vein endothelial cells via mitochondrial dysfunction and endoplasmic reticulum stress. *Oxid. Med. Cell Longev.* 2017: 5736506. doi:10.1155/2017/5736506

\*Corresponding author; email: choykerwoon@uitm.edu.my